

Superplastic Alumina Ceramics with Grain Growth Inhibitors

Liang A. Xue,* Xin Wu,* and I-Wei Chen*

Department of Materials Science and Engineering, The University of Michigan, Ann Arbor, Michigan 48109-2136

Superplastic deformation of alumina ceramics was studied at 1400° to 1450°C and at a strain rate of 4×10^{-5} to 5×10^{-4} s⁻¹. MgO and ZrO₂ were introduced to suppress dynamic grain growth. The latter was especially effective; grain growth was minimal in 10-vol%-ZrO₂-containing material. Both materials were superplastically stretched under biaxial tension to 100% engineering strain with good surface finishing, demonstrating the feasibility of superplastic forming for alumina ceramics. [Key words: alumina, superplastic, deformation, grain growth, additives.]

I. Introduction

IN A previous paper,¹ we showed that, for pure alumina, grain growth during sintering was effectively suppressed through low-temperature sintering. Nevertheless, dynamic grain growth occurred rapidly in superplastic deformation. The latter had a devastating effect on the superplastic behavior of the material. Although the aforementioned ultra-fine-grained pure alumina exhibited rather low initial flow stresses at relatively low temperatures and hence might have been a good candidate for superplastic ceramic, this was not realized because the dynamic grain growth caused strain-hardening leading to cavitation and cracking. Therefore, it became clear that the control of dynamic grain growth was an essential next step in the development of superplastic alumina ceramics.

The phenomenon of dynamic grain growth during superplastic deformation of fine-grained ceramics has been well documented.²⁻⁷ However, its cause and remedy are not yet clear. Following the previous work in the literature on sintering and static grain growth, we have added MgO⁸ and ZrO₂⁹ to alumina in an attempt to lower the grain-boundary mobility through solute drag (MgO) or second-phase pinning (ZrO₂),¹⁰ thereby suppressing dynamic grain growth. These approaches have proved successful. As a result, superplastic alumina ceramics deformable under biaxial tension have been obtained.

II. Experimental Procedure

The procedure for material preparation was essentially the same as that reported previously,¹ except for an additional step of introducing additives to pure alumina. This was done by adding an aqueous solution of either Mg(NO₃)₂ or ZrOCl₂ to a dispersed suspension of alumina powders in distilled water. The pH of the mixture was then adjusted to floc the suspension. The amount of MgO introduced was 200 ppm, a

value around the solubility limit.¹¹ The volume fraction of ZrO₂ addition was 10% (ZrO₂ and Al₂O₃ have little solubility for each other). The slurry was dried and calcined (700°C for MgO-doped alumina and 1000°C for ZrO₂-containing alumina). The powder thus obtained was again milled, dispersed and pressure-cast into cakes as described elsewhere.¹² The sintering temperatures used were 1320°C for MgO-doped alumina and 1480°C for ZrO₂-added alumina, compared to 1250°C for pure alumina. A final density of greater than 98% of the theoretical was reachable in 2 h (4 h in the case of pure alumina). Other experimental procedures for specimen preparation, compression testing, superplastic stretching, and microstructural characterization were the same as reported previously.^{1,12,13} For ZrO₂-added alumina, the average linear intercept length was corrected for a second phase using the method of Wurst and Nelson.¹⁴

III. Results and Discussion

(1) Sintered Microstructures

Polished cross sections of sintered samples of pure alumina, MgO-doped alumina, and ZrO₂-added alumina are shown in Figs. 1(A), (B), and (C), respectively. Both undoped and MgO-doped aluminas show typical microstructures of a single-phase material, although the grain size distribution in undoped alumina appears somewhat wider. In ZrO₂-added material, small ZrO₂ inclusions are well distributed, lying almost exclusively at alumina grain triple junctions. The average grain sizes of these specimens were 0.51 μm for undoped, 0.53 μm for MgO-doped, and 0.50 μm for ZrO₂-added alumina. Apparently, during low-temperature sintering, grain size seems not to have been further reduced by these additives. (As shown previously, static grain growth in alumina at temperatures below 1300°C was already very slow.)

(2) Effect of Additives on Deformation and Grain Growth

True stress versus true strain curves at 1400°C and a constant strain rate of 10⁻⁴/s in compression are shown in Fig. 2 for pure, MgO-doped, and ZrO₂-added alumina. Extensive strain hardening was evident only for pure alumina. As discussed in the previous paper,¹ the strain hardening can be attributed to dynamic grain growth. (The drop of stress at large strain is due to severe cavitation which is more pronounced here than that at lower temperature and lower strain rate.) Compared to pure alumina, strain hardening for MgO-doped alumina is modest; its flow stress increased from an initial value of about 20 MPa to some 50 MPa after a deformation strain of 0.68. Strain hardening can be totally suppressed by 10% ZrO₂ addition. Indeed, although the initial flow stress of ZrO₂-containing alumina is the highest, it becomes comparable to those of the other two aluminas at large strains.

Data of flow stress and strain rate at 1400°C for undoped, MgO-doped, and ZrO₂-added alumina are summarized in Fig. 3. Because of pronounced dynamic grain growth in pure alumina, flow stress at 2% strain was used here for comparison. Since the initial grain sizes were nearly the same for the three materials, these data can be compared directly with each other. A common feature of these data is a stress expo-

R. Raj—contributing editor

Manuscript No. 197355. Received August 17, 1990; approved December 7, 1990.

Presented at the 92nd Annual Meeting of the American Ceramic Society, Dallas, TX, April 23, 1990 (Paper No. 5-JV-90).

Supported by the U. S. Army Research Office under Contract No. DAALO3-89-KO133.

*Member, American Ceramic Society.

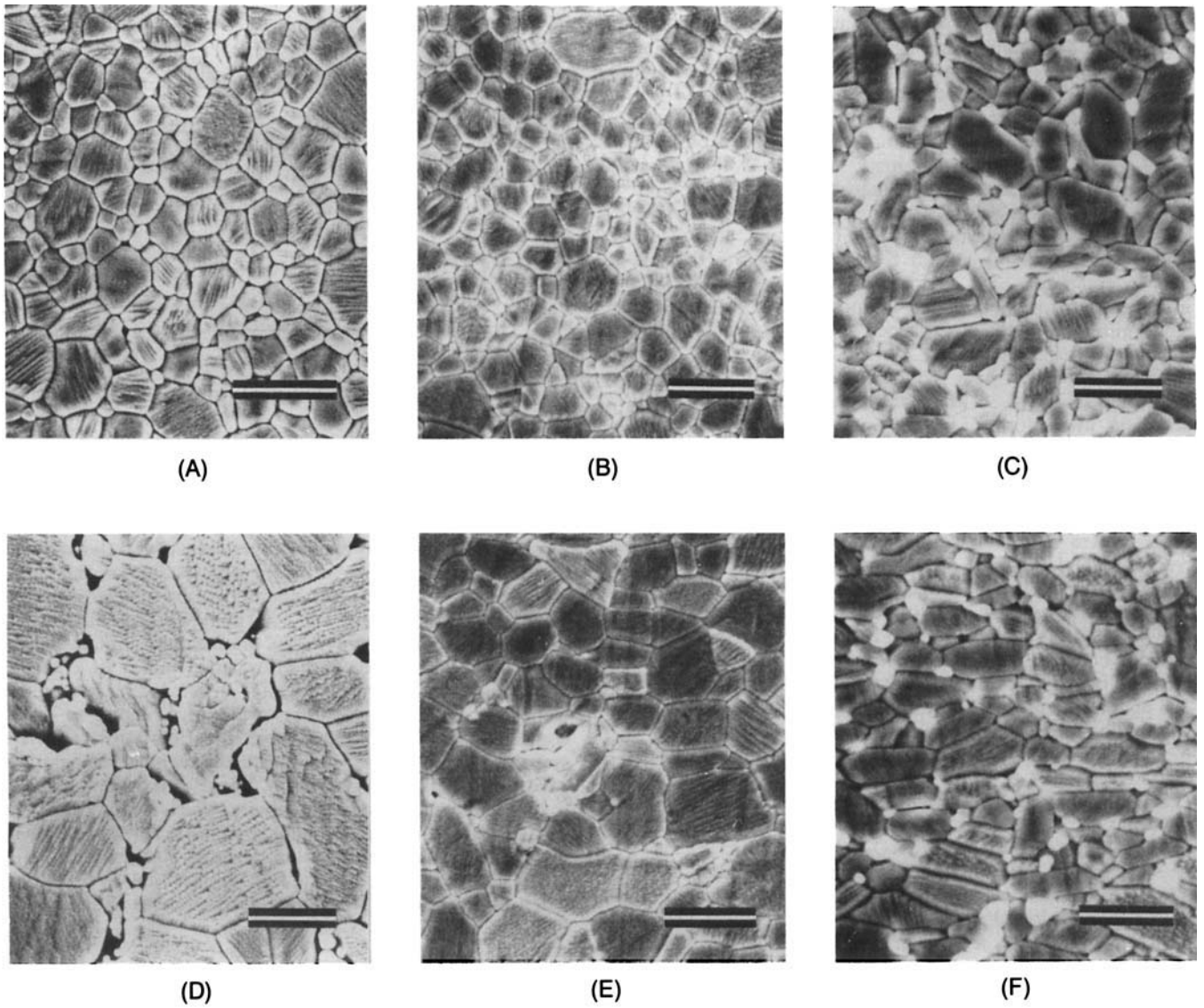


Fig. 1. Scanning electron micrographs of polished cross sections of various aluminas (bar = 1 μm). As-sintered specimens: (A) pure; (B) MgO-doped; (C) ZrO₂-added. Deformed at 1400°C, 10⁻⁴/s: (D) pure, $\epsilon = 0.57$; (E) MgO-doped, $\epsilon = 0.68$; (F) ZrO₂-added; $\epsilon = 0.68$.

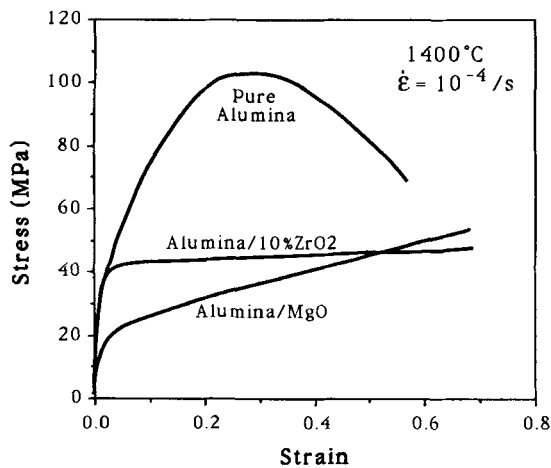


Fig. 2. Flow stress at a constant strain rate of 10⁻⁴/s versus strain curves for pure, MgO-doped, and ZrO₂-added alumina.

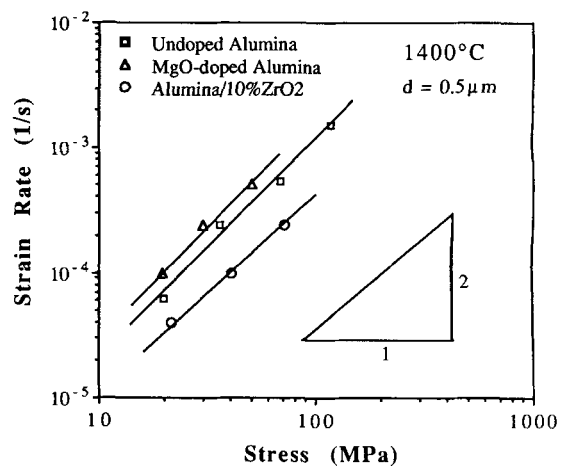


Fig. 3. Relationship between strain rate and flow stress at 2% strain at 1400°C for pure, MgO-doped, and ZrO₂-added alumina.

ment near 2. This would suggest that the additives do not change the deformation mechanism of alumina if the same microstructure is maintained under these deformation conditions. A small increase of strain rate due to MgO is observed, as is the depression of strain rate due to ZrO_2 . These observations are in agreement with Cannon *et al.*'s work on pure and MgO-doped fine-grained alumina,¹⁵ and with Wakai *et al.*'s study on pure and ZrO_2 -added alumina.¹⁶

The corresponding microstructures of these materials after deformation are shown in Figs. 1(D) (undoped), 1(E) (MgO-doped), and 1(F) (ZrO_2 -added). Extensive grain growth is evident by comparing Figs. 1(A) and (D) for pure alumina. The grain growth for MgO-doped alumina is less pronounced. The grain size in the ZrO_2 -added material remains almost unchanged despite its change in the aspect ratio.

The evolution of grain size during deformation is further illustrated in Fig. 4, in which the normalized alumina grain size data, in the form of $\ln(d/d_0)$, are plotted against strain. Here d is the current grain size and d_0 is the initial grain size. Also included are the two datum points of Mocellin *et al.*⁵ and the data of Venkatachari and Raj¹⁷ for MgO-doped alumina of a coarser grain size. These data clearly show the grain growth retardation effect of MgO and ZrO_2 . For the case of MgO doping, the data from three independent studies are generally in agreement with each other. However, the data of Venkatachari and Raj show somewhat less grain growth than those found in the present study and in Mocellin *et al.*'s work. This is not surprising since in the former the amount of MgO employed was 0.25 wt% in contrast to 200 ppm in the present study and 500 ppm in Mocellin *et al.*'s work. (The former concentration is well over the solubility of MgO in alumina,¹¹ thus second-phase pinning may well be operative.)

Static grain growth also occurred to some extent during the deformation. This can be noted from the data in Fig. 4; none of these lines except that of ZrO_2 -added alumina seems to pass the origin. Nevertheless, the main contribution to the grain size increase was from dynamic grain growth. For example, for undoped alumina of an initial grain size of $0.51 \mu\text{m}$ at 1400°C , a deformed specimen (strain rate = $3 \times 10^{-4}/\text{s}$ for $2 \times 10^3 \text{ s}$) has $d = 1.6 \mu\text{m}$, while an annealed specimen reached $d = 0.9 \mu\text{m}$ over the same time period. In the case of MgO-doped alumina at 1420°C ,¹⁷ deformation to a strain of 0.66 increased grain size from 1.6 to $3.05 \mu\text{m}$, whereas in the same period (186 min), the grain size of an annealed sample reached only $1.8 \mu\text{m}$.

Finally, to investigate the cause of elongated grains formed during deformation of ZrO_2 -added material, we have per-

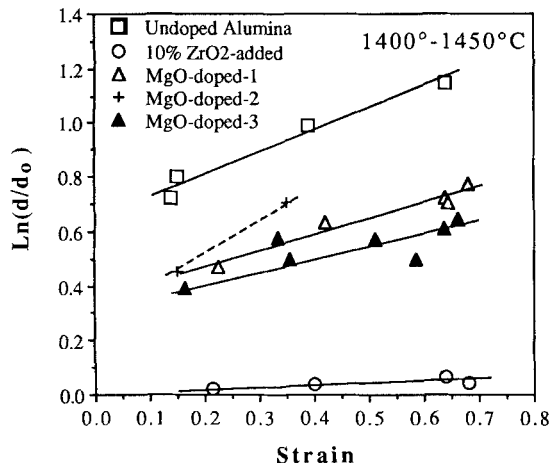


Fig. 4. Normalized grain size (see text) versus strain for various aluminas. Data of MgO-doped-1 are of this study, those of MgO-doped-2 are of Mocellin *et al.* (Ref. 5, $d_0 = 1.17 \mu\text{m}$), and those of MgO-doped-3 are of Venkatachari and Raj (Ref. 17, $d_0 = 1.6 \mu\text{m}$).

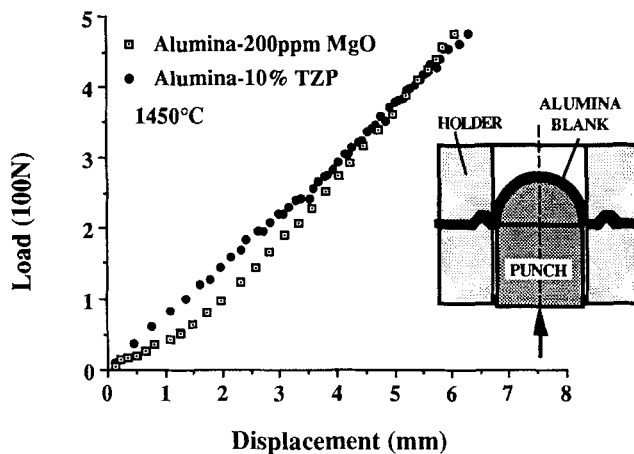


Fig. 5. Forming load versus punch displacement for MgO-doped and ZrO_2 -added alumina during superplastic stretching at 1450°C . The average strain rate is $3 \times 10^{-4}/\text{s}$ for the former and $1.5 \times 10^{-4}/\text{s}$ for the latter.

formed additional deformation experiments over a wide range of strain rate and temperature to large strains on the three aluminas shown in Fig. 1. In addition, a ZrO_2 -added alumina which was further doped with 1000 ppm MgO was also tested. We have found that the extent of grain elongation was consistent with the magnitude of the flow stress. Thus, for example, at a constant strain rate and total strain, grains were more elongated at lower temperatures, while MgO doping to ZrO_2 -containing alumina lowered both the flow stress and the grain elongation. At the same flow stress, a higher temperature gave rise to a larger aspect ratio. These observations suggest that an increased dislocation activity, which is more sensitive to flow stress than diffusional superplastic flow, is probably responsible for grain elongation, and the higher aspect ratio of ZrO_2 -added alumina is due to its higher flow stress during much of the earlier stage of deformation as indicated in Fig. 2.

(3) Superplastic Stretching

We have verified the superplastic formability of MgO-doped and ZrO_2 -added alumina, using the punch bulging test described elsewhere.¹³ In this test, a flat disk is stretched by a semispherical punch to a dome shape. When the height of the dome reaches the same as the dome radius, the surface area is approximately twice that of the original. This corresponds to a biaxial engineering strain of 100%.

Typical curves of forming load versus punch displacement for MgO-doped and ZrO_2 -added aluminas at 1450°C are

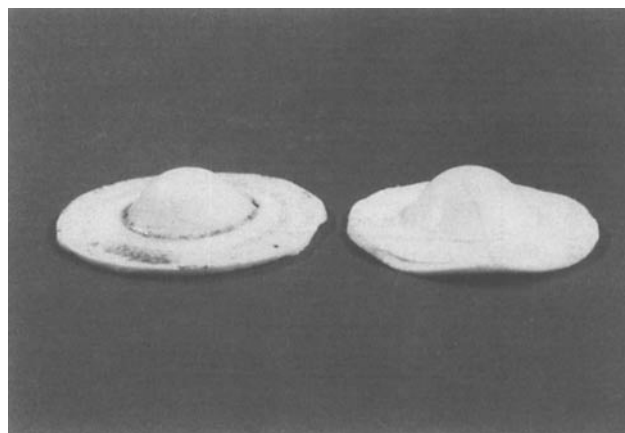


Fig. 6. Superplastic-stretched alumina disks: (left) MgO-doped; (right) ZrO_2 -added.

shown in Fig. 5. The punch radius used was 6.5 mm. The average strain rate was 3×10^{-4} /s for MgO-doped alumina and 1.5×10^{-4} /s for ZrO₂-added alumina. The increase in load with the displacement in the case of ZrO₂-added sample is due essentially to the increase in the deforming area of the specimen, since grain growth/strain hardening is negligible in this material. In comparison, the MgO-doped sample showed a lower load in the early stage but a more rapid load increase at the later stage, which is consistent with its lower initial flow stress and faster dynamic grain growth as already discussed earlier.

In both cases, full stretching to a half-spherical-shaped dome was successfully completed. Figure 6 shows photographs of two punch-stretched specimens, with MgO-doped alumina on the left and ZrO₂-added alumina on the right. The quality of the as-formed surfaces is good. This demonstrates that, once dynamic grain growth is suppressed, deformation processing of alumina ceramics should be feasible.

References

- ¹L. A. Xue and I-W. Chen, "Deformation and Grain Growth of Low-Temperature-Sintered High-Purity Alumina," *J. Am. Ceram. Soc.*, **73** [11] 3518-21 (1990).
- ²F. Wakai, S. Sakaguchi, and H. Kato, "Compressive Deformation Properties and Microstructures in the Superplastic Y-TZP," *J. Ceram. Soc. Jpn.*, **94**, 72-75 (1986).
- ³L. A. Xue and R. Raj, "Superplastic Deformation of Zinc Sulfide near Its Transformation Temperature (1020°C)," *J. Am. Ceram. Soc.*, **72** [10] 1792-96 (1989).
- ⁴T.-G. Nieh and J. Wadsworth, "Dynamic Grain Growth During Superplastic Deformation of Yttria-Stabilized Tetragonal Zirconia Polycrystals," *J. Am. Ceram. Soc.*, **72** [8] 1469-72 (1989).
- ⁵J. D. Fridez, C. Carry, and A. Mocellin, "Effects of Temperature and Stress on Grain-Boundary Behavior in Fine-Grained Alumina"; pp. 720-40 in *Advances in Ceramics, Vol. 10, Structure and Properties of MgO and Al₂O₃ Ceramics*. Edited by W. D. Kingery. American Ceramic Society, Columbus, OH, 1984.
- ⁶C. Carry and A. Mocellin, "Example of Superplastic Forming Fine-Grained Al₂O₃ and ZrO₂ Ceramics"; pp. 1043-1052 in *High Tech Ceramics*. Edited by P. Vincenzini. Elsevier Science Publishers B.V., Amsterdam, Netherlands, 1987.
- ⁷C. Carry and A. Mocellin, "Structural Superplasticity in Single Phase Crystalline Ceramics," *Ceram. Int.*, **13**, 89-98 (1987).
- ⁸S. J. Bennison and M. P. Harmer, "Grain-Growth Kinetics for Alumina in the Absence of a Liquid Phase," *J. Am. Ceram. Soc.*, **68** [1] C-22-C-24 (1985).
- ⁹F. F. Lange and M. M. Hirlinger, "Hindrance of Grain Growth in Al₂O₃ by ZrO₂ Inclusions," *J. Am. Ceram. Soc.*, **67** [3] 164-68 (1984).
- ¹⁰R. J. Brook, "Controlled Grain Growth," *Treatise Mater. Sci. Technol.*, **9**, 331-64 (1976).
- ¹¹S. K. Roy and R. L. Coble, "Solubilities of Magnesia, Titania and Magnesium Titanate in Aluminum Oxide," *J. Am. Ceram. Soc.*, **51** [1] 1-6 (1968).
- ¹²C.-M. J. Hwang and I-W. Chen, "Effect of a Liquid Phase on Superplasticity of 2-mol%-Y₂O₃-Stabilized Tetragonal Zirconia Polycrystals," *J. Am. Ceram. Soc.*, **73** [6] 1626-32 (1990).
- ¹³X. Wu and I-W. Chen, "Superplastic Bulging of Fine-Grained Zirconia," *J. Am. Ceram. Soc.*, **73** [3] 746-49 (1990).
- ¹⁴J. C. Wurst and J. A. Nelson, "Lineal Intercept Technique for Measuring Grain Size in Two-Phase Polycrystalline Ceramics," *J. Am. Ceram. Soc.*, **55** [2] 109 (1972).
- ¹⁵R. M. Cannon, W. H. Rhodes, and A. H. Heuer, "Plastic Deformation of Fine-Grained Alumina (Al₂O₃): I. Interface-Controlled Diffusional Creep," *J. Am. Ceram. Soc.*, **63** [1-2] 46-53 (1980).
- ¹⁶F. Wakai, T. Iga, and T. Nagano, "Effect of Dispersion of ZrO₂ Particles on Creep of Fine-Grained Al₂O₃," *J. Ceram. Soc. Jpn.*, **96** [12] 1206-209 (1988).
- ¹⁷K. R. Venkatachari and R. Raj, "Superplastic Flow in Fine-Grained Alumina," *J. Am. Ceram. Soc.*, **69** [2] 135-38 (1986). □